THE JOURNAL OF BIOLOGICAL CHEMISTRY VOL. 288, NO. 6, pp. 4475–4485, February 8, 2013

Interactions of *Anopheles gambiae* Odorant-binding Proteins with a Human-derived Repellent

*IMPLICATIONS FOR THE MODE OF ACTION OF N,N-DIETHYL-3-METHYLBENZAMIDE (DEET)**

Received for publication, November 14, 2012, and in revised form, December 20, 2012 Published, JBC Papers in Press, December 23, 2012, DOI 10.1074/jbc.M112.436386

Emma J. Murphy[‡], Jamie C. Booth[§], Foteini Davrazou[‡], Alex M. Port[‡], and David N. M. Jones[‡§1]

From the [‡]Department of Pharmacology and the [§]Program in Structural Biology and Biophysics, University of Colorado School of Medicine, Aurora, Colorado 80045

Background: Odorant-binding proteins mediate recognition of odors that guide mosquito behavior.
Results: Studies of AgamOBP1 reveal the binding site for the natural repellent 6-methyl-5-hepten-2-one (6-MH).
Conclusion: 6-MH binds to the same site as DEET and blocks the interaction of AgamOBP1 with other OBPs.
Significance: In targeting OBPs in mosquitoes, the location of repellent binding may count more than the binding affinity.

The *Anopheles gambiae* mosquito, which is the vector for *Plasmodium falciparum* malaria, uses a series of olfactory cues emanating from human sweat to select humans as their source for a blood meal. Perception of these odors within the mosquito olfactory system involves the interplay of odorant-binding proteins (OBPs) and odorant receptors and disrupting the normal responses to those odorants that guide mosquito-human interactions represents an attractive approach to prevent the transmission of malaria. Previously, it has been shown that DEET targets multiple components of the olfactory system, including OBPs and odorant receptors. Here, we present the crystal structure of *A. gambiae* OBP1 (OBP1) in the complex it forms with a natural repellent 6-methyl-5-heptene-2-one (6-MH). We find that 6-MH binds to OBP1 at exactly the same site as DEET. However, key interactions with a highly conserved water molecule that are proposed to be important for DEET binding are not involved in binding of 6-MH. We show that 6-MH and DEET can compete for the binding of attractive odorants and in doing so disrupt the interaction that OBP1 makes with OBP4. We further show that 6-MH and DEET can bind simultaneously to OBPs with other ligands. These results suggest that the successful discovery of novel reagents targeting OBP function requires knowledge about the specific mechanism of binding to the OBP rather than their binding affinity.

The *Anopheles gambiae* mosquito is the primary vector for the human malaria parasite *Plasmodium falciparum* that is responsible for more than one million deaths annually (1). Female *A. gambiae* have an extremely high preference for feeding on human hosts. The problems of drug resistance to established drugs and the emergence of resistance to artemisinin-based therapies (2), combined with the limited efficacy of vaccines (3), suggest that approaches that reduce the contact between mosquitoes and their human host will remain as important approaches in combating the transmission of malaria (4).

The selectivity of the female mosquito for human hosts is guided by olfactory responses to odor molecules that emanate from human skin and sweat (5). Individuals vary in their intrinsic attractiveness to mosquitoes (6, 7), and one of the main reasons for this may be the differences in the composition of human sweat (8). Several compounds have been identified in human sweat which may contribute to the avoidance of certain people by mosquitoes (9). One of these compounds, 6-methyl-5-hepten-2-one (6-MH),[2] has been shown to repel mosquitoes in arm-in-cage testing (10) and is also used in many plant-based or natural repellents (11).

The perception of odorants in insects occurs predominantly in the olfactory sensilla. Within these specialized structures, odorant-binding proteins (OBPs), expressed by specialized support cells, are secreted into the lymph fluid that surrounds the olfactory dendrites (12). These OBPs are present in high concentrations (millimolar) (13) and are one of the first components of the olfactory system to come into contact with airborne odorants and repellents. OBPs are proposed to have multiple roles including protection of odorants from odorant-degrading enzymes, and transporting hydrophobic odor molecules through the lymph fluid to membrane-bound odorant receptors. There is evidence that OBPs function as passive carriers (14–18) but in some cases have a more direct role where formation of a specific odorant-OBP complex is required for odorant receptor activation (19–21).

Disruption of the normal olfactory responses to odor molecules that control mosquito behavior provides a means to reduce human-mosquito interactions; a primary method for

* This work was supported, in whole or in part, by National Institutes of Health Grant DC008834 (to D. N. M. J.).
The atomic coordinates and structure factors (code 4FQT) have been deposited in the Protein Data Bank (http://wwpdb.org/).
[1] To whom correspondence should be addressed: Dept. of Pharmacology, University of Colorado School of Medicine, 12801 East 17th Ave., Aurora, CO 80045. Tel.: 303-724-3600; Fax: 303-724-3663; E-mail: david.jones@ucdenver.edu.

[2] The abbreviations used are: 6-MH, 6-methyl-5-hepten-2-one; Bistris propane, 1,3-bis[tris(hydroxymethyl)methylamino]propane; DEET, *N,N*-diethyl-3-methylbenzamide; HSQC, heteronuclear single quantum coherence; 1-NPN, *N*-phenyl-*1*-naphthylamine; 1,8-ANS, 1-anilinonaphthalene-8-sulfonic acid; OBP, odorant-binding protein; PDB, Protein Data Bank.

achieving this is the use of repellents. *N,N*-Diethyl-3-methylbenzamide (DEET) is considered the most broad spectrum and effective insect repellent available (22). Although effective, DEET is also known to be toxic (23), to have reduced efficacy with time after application, and to be ineffective against species that develop resistance (24). The need for a new, more effective, and less toxic repellent is evident, and to develop a new repellent the mechanism of their action must first be elucidated. Despite its widespread use, the mechanism of action and molecular targets of DEET are still the subject of some debate. It has been shown that DEET blocks electrophysiological responses of olfactory sensory neurons to odors in *A. gambiae* and *Drosophila melanogaster* (25). It has been proposed that DEET can prevent normal interactions of odorants with the olfactory receptor to block host odor recognition, although the exact mechanism that underlies this is not clear (26). Alternatively, it has been proposed that DEET functions to activate olfactory neurons that elicit avoidance behavior (27). Recent studies have provided evidence that DEET can also interact directly with OBPs, including OBP1 (28). Previous work has established that OBP1 is required for olfactory responses to indole and 3-methyl-indole, which are major components of incubated human sweat (29) and that the formation of a heterodimeric interaction between OBP1 and 4, which co-localizes with OBP1, may be important for the increased binding affinity of odorants (30). We have recently shown that the heterodimeric interaction between OBP1 and 4 requires indole (31). Therefore, DEET acting on OBPs to disrupt the interactions that they make with other OBPs or other components of the olfactory system could disrupt downstream activation of odorant receptors.

Here, we present the crystal structure of OBP1 bound to 6-MH, which reveals that this natural repellent binds at the same site as DEET. We use NMR spectroscopy to show that OBP1 does not interact with OBP4 in the presence of 6-MH or DEET and that addition of 6-MH to the OBP1-indole-OBP4 complex disrupts this interaction. We propose that repellents such as DEET and 6-MH may function to prevent OBP heterodimerization and so inhibit odor recognition. Our results suggest evidence for a complex interplay between OBPs and their ligands and that attraction and repulsion may be controlled by conformational changes in OBPs and the interactions that they facilitate.

EXPERIMENTAL PROCEDURES

Protein Expression and Purification—OBP1 and 4 were expressed and purified as described previously (32, 33) and verified by mass spectroscopy. For NMR experiments, proteins were isotopically labeled by expression in minimal media containing ^{15}N-labeled ammonium chloride (99 atom %).

NMR Spectroscopy—Samples for NMR were made in 20 mM sodium phosphate at pH 7.4 containing 10% D_2O. All NMR spectra were recorded on a Varian 600 MHz spectrometer.

^{15}N T_1 and T_2 Relaxation Measurements—^{15}N T_1 and T_2 relaxation measurements were acquired using the standard pulse sequences supplied by the manufacturer. For these measurements the T_1 relaxation delay time was varied between 10 and 1300 ms, and T_2 relaxation times between 10 and 210 ms with a recycle delay of 3.5 s between each scan. Values of the individual relaxation time constants for each residue were obtained by fitting the intensities of each peak as a function of the delay time to a standard exponential decay in CcpNmr Analysis 2.2.2 (34, 35). The overall correlation time was then calculated from the average T_1/T_2 ratio of those residues in ordered regions of secondary structure, according to Equation 1, where ν_N is the NMR frequency of the ^{15}N nucleus in hertz. The resulting value was then compared with established correlation times for well characterized monomeric globular proteins of varying molecular mass (36). Subsequently for the OBP1-DEET complex, an estimate of the correlation time was obtained from a fit of global T_1 and T_2 relaxation times using one-dimensional versions of the ^{15}N relaxation experiments as described previously (37) by fitting the integrated signal intensity from backbone amides in the amide ^{1}H region as a function of delay time to an exponential decay. Each experiment was repeated three times.

$$\tau_c \approx \frac{1}{4\pi\nu_N}\sqrt{6\frac{T_1}{T_2} - 7} \qquad \text{(Eq. 1)}$$

Crystallization and X-ray Data Collection and Refinement—OBP1 crystals were grown in 100 mM Bistris propane, pH 8.78, 31% polyethylene glycol (PEG) 4000 at 4 °C. Both the protein and well solution were saturated with 6-MH prior to crystallization. X-ray diffraction data were collected at the Molecular Biology Consortium Beamline 4.2.2 (wavelength = 1.0 Å) at the Advanced Light Source at Lawrence Berkeley National Laboratory, Berkeley, CA. Data sets for OBP1 were processed using d*Trek (38). The crystal structure was solved by molecular replacement starting from the published structure of OBP1 (PDB 2ERB) using Phaser (39) within the CCP4 suite (40) and refined using Refmac5 (41) followed by manual rebuilding in COOT (42).

Fluorescence Spectroscopy—To measure the affinity of the fluorescent probes, 1-NPN and 1,8-ANS, protein solutions of between 0.1 and 1.0 μM in 50 mM Tris-HCl, pH 7.4, were titrated with the probe (1 mM in methanol) to final concentrations of $\approx$ 16 μM (1-NPN) and $\approx$ 60 μM (1,8-ANS). Emission fluorescence spectra were recorded on a Horiba Fluorolog-3 spectrofluorometer at 25 °C in a 1-cm path length cuvette. For 1-NPN an excitation wavelength of 337 nm was used, and emission spectra were recorded between 380 and 600 nm, for 1,8-ANS the excitation wavelength used was 380 nm, and spectra were recorded between 400 and 600 nm. Emission was recorded at 1-nm intervals with an integration time of 0.5 s and slit widths of 5 nm for both probes.

To determine the K_D for probe binding, the fluorescence intensity (cps) at the emission maxima (408 nm for OBP1–1-NPN, 402 nm for OBP4–1-NPN, and 456 nm for both OBP1–1,8-ANS and OBP4–1,8-ANS) was plotted against the total concentration of probe and the resulting curves were fit using Equation 2. This is an explicit solution to the binding equation and accounts for ligand depletion where free ligand cannot be equated to total ligand concentration (43). In this equation F_{max} is the maximum emission intensity of the bound reporter, the term A gives the concentration of the bound protein, P is the

total protein concentration, L is the total probe concentration, and I is the concentration of any competitor. Equation 2 includes a correction for the fluorescence from excess free probe, F_{lig}, which is the maximum emission intensity of the free probe at the emission wavelength of the bound state of the probe. This was determined by titration of probe into binding buffer and is in units of cps per μM of free probe. We assumed that the protein is 100% active and that the protein:probe stoichiometry is 1:1. This assumption is based on crystal structures of other OPBs that show a single molecule of 1-NPN (44) and 1,8-ANS (45) bound to these proteins. Under these assumptions, the term A also represents the concentration of bound ligand. For experiments performed in the absence of any competitor, K_{app} simplifies to K_D for the ligand. All experiments were repeated at least three times, and the values reported are the mean ± S.D.

K_i values for ligands were determined in two ways. To confirm that binding of ligands is competitive for binding of probe, assays were performed by titrating the fluorescent probe into protein in the presence of increasing concentrations of ligand. OBPs were incubated with ligand competitor at 25 °C for 30 min prior to probe titration. If binding was directly competitive, binding data were simultaneously fit for all concentrations of the competing ligand to Equation 2, where K_D and K_i were shared across each individual data set (Equations 3 and 4). Alternatively, fluorescent probe displacement assays were carried out by titrating ligand into samples of the protein-probe complex. For 1-NPN displacement assays OBPs (1 μM OBP1 or 0.5 μM OBP4) were incubated with equimolar 1-NPN for 30 min at 25 °C. Ligands (10 mM in methanol) were titrated in to final concentrations of ~150 μM and the change in fluorescence intensity recorded. EC_{50} values were calculated by fitting plots of fluorescence intensity at the emission wavelength of the bound probe as a function of ligand concentration to a one-site binding model using GraphPad Prism, version 5.0a. The Cheng-Prusoff correction (Equation 5) was used to convert EC_{50} to K_i. 1,8-ANS displacement assays were carried out in the same way using 5 μM protein and 20 μM 1,8-ANS. All binding experiments were repeated three times and the values reported are the mean ± S.D.

$$F = F_{max}\frac{A}{P} + F_{lig}(L - A) \quad \text{(Eq. 2)}$$

where

$$A = \frac{(K_{app} + L + P) - \sqrt{(K_{app} + L + P)^2 - 4PL}}{2} \quad \text{(Eq. 3)}$$

and

$$K_{app} = K_D\left(1 + \frac{[I]}{K_i}\right) \quad \text{(Eq. 4)}$$

$$K_i = EC_{50}\Big/\left(1 + \frac{L}{K_L}\right) \quad \text{(Eq. 5)}$$

RESULTS

Crystal Structure of OBP1–6-MH Complex—The crystal structure of the OBP1–6-MH complex (PDB 4FQT) was solved to a 2.2 Å resolution (Fig. 1 and Table 1) with final values of R_{work} and R_{free} of 18.4 and 23.8%, respectively. As described previously (46) the overall fold of OBP1 is similar to that of other OBPs with six α-helices connected with three disulfide bridges. The crystal contains two protein molecules per asymmetric unit with a dimeric interface being formed across the noncrystallographic 2-fold axis that buries ~1200 Å^2 of surface area. The OBP1–6-MH complex resembles both the previous structure of OBP1 bound to PEG (PDB 2ERB) (46) and the OBP1-DEET complex (PDB 3N7H) (28), with root mean square deviations of the backbone atoms of 0.41 Å and 0.43 Å (OBP1-PEG and OBP1-DEET, respectively). In the original structure of OBP1 bound to PEG (2ERB), there was continuous electron density that defined the location of a single PEG molecule that crosses between the two monomers of the asymmetric unit in what has been described as a hydrophobic tunnel (46). In contrast, in the structure described here, the electron density is not continuous but shows distinctive breaks in the region of the tunnel at the interface between the two molecules in the asymmetric unit. An $F_o - F_c$ omit map clearly shows two areas of unconnected flattened density which can be modeled as 6-MH. Even in the structures refined in the presence of 6-MH, there is no indication of any additional density between the density defining the 6-MH and the adjacent PEG molecule (see below). In further support of this structure, we also obtained multiple crystals of OBP1 in the absence of 6-MH and in these cases the electron density in the "tunnel" is continuous, consistent with the presence of PEG binding (data not shown) as observed in the original structure of OBP1 (46). This gives further confidence that the density we observe in the present structure originates from 6-MH.

6-MH Binds in the Same Binding Pocket as DEET—One 6-MH molecule is bound to each subunit of the OBP1 dimer, close to the interface between the two subunits (Fig. 1*A*). The binding pocket for 6-MH is formed by residues belonging to helix 4 (Leu-73, Leu-76, Leu-80, and His-77), helix 5 (Ala-88, Met-89, Met-91, and Gly-92) and helix 6 (Trp-114), as described previously for the binding pocket of DEET (28). In the OBP1-DEET structure a water molecule bridges interactions between DEET and the indole group of Trp-114 (Fig. 1*B*), and it has been proposed that this water is important for repellent binding. This water is conserved in the present structure with 6-MH but is not involved in bridging any interactions between the ligand and the protein (Fig. 1*C*). Therefore, it appears unlikely to play a significant role in ligand binding. In addition to 6-MH, each subunit of the present structure also binds a molecule of PEG, from the crystallization conditions, in the central binding pocket, a PEG molecule is also observed in each subunit of the OBP1-DEET structure in the same place (28).

OBP4 Does Not Interact with OBP1 in the Presence of 6-MH or DEET—Recent studies have implicated heterodimeric interactions between OBP1 and OBP4 as important for odor perception (29, 30). Therefore, we used NMR spectroscopy to test the effects of 6-MH on the interaction between OBP1 and OBP4.

We recorded two-dimensional ^{1}H-^{15}N heteronuclear single quantum coherence (HSQC) NMR spectra of OBP1 in the absence and presence of 6-MH. The spectrum of apo-OBP1 recorded at pH 7.4 contains 100 of an expected 116 peaks, indi-

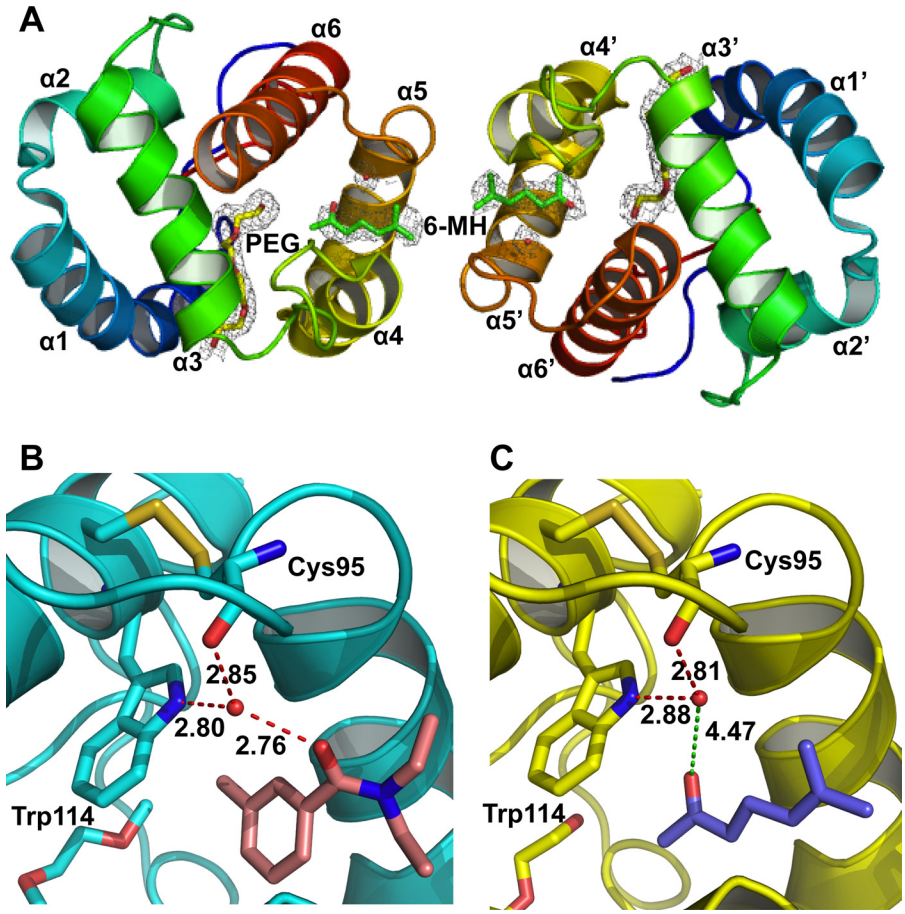

FIGURE 1. **Crystal structure of the OBP1–6-MH complex.** *A*, schematic representation of the overall structure of the OBP1 dimer showing two molecules of 6-MH (*green*) bound at the interface and two molecules of PEG (*yellow*) filling the rest of the binding pocket. The density from a $2F_o - F_c$ map is contoured at 1 σ in *gray*, and waters are shown in *red*. *B*, schematic representation of the OBP1-DEET complex. Hydrogen bonds between DEET (*salmon*), Trp-114, Cys-95, and a water molecule are shown in *red* and labeled with interatomic distances (Å). *C*, schematic representation of the OBP1–6-MH complex. The carbonyl group of 6-MH (*blue*) is 4.47 Å away from the conserved water molecule and so is not within hydrogen bonding distance. The water molecule that is conserved in all three OBP structures published to date is shown in *red*.

TABLE 1

Data collection and refinement statistics (molecular replacement)

Single crystal. Values in parentheses are for highest resolution shell.

Crystal parameters	OBP1–6-MH (PDB ID 4FQT)
Space group	P1 2_1 1
Cell dimensions	
a, *b*, *c* (Å)	32.77, 68.99, 64.52
α, β, γ (°)	90.0, 104.71, 90.0
Data collection	
Resolution (Å)	31.70–2.20 (2.3699–2.2001)
R_{merge}	0.095 (0.310)
$I/\sigma I$	7.41 (3.17)
Completeness (%)	99.17 (98.51)
Redundancy	3.50 (3.19)
Refinement statistics	
Resolution (Å)	2.20
No. reflections	14,068 (1,450)
R_{work} (%)/R_{free} (%)	18.51/23.89 (31.22/37.31)
No. atoms	
Protein	4,370
Ligand/ion	45
Water	170
Average *B*-factor (Å^2)	32.3
Root mean square deviations	
Bond lengths (Å)	0.010
Bond angles (°)	1.419

cating that the protein is relatively well ordered in the absence of ligand (31). In the presence of 6-MH we see a number of chemical shift changes consistent with binding of 6-MH to OBP1 (Fig. 2*A*). As reported previously (31), apo-OBP4 is a monomer in solution, but the NMR spectrum contains only 35 (of an expected 114) intense, well resolved peaks from backbone amides. The remaining peaks are broadened or not detectable, indicative of significant conformational averaging occurring on the micro- to millisecond time scale. The addition of 6-MH to OBP4 induces a dramatic improvement in the appearance of the spectrum such that we now observe 107 peaks (Fig. 2*B*). We observed a similar result for OBP4 with indole (31), and for ligand binding to the *Drosophila* OBP LUSH (32, 47).

When OBP4 is added to ^{15}N-labeled OBP1 in the presence of indole there are significant chemical shift changes in the spectrum of OBP1 indicative of an interaction between the two proteins (31). In contrast, when OBP4 is added to the ^{15}N-OBP1–6-MH complex there are no significant changes in the spectrum of OBP1 (Fig. 2*A*). Similarly, we observe no changes in the spectrum of the ^{15}N-OBP4–6MH complex when unlabeled OBP1 is added to the sample (Fig. 2*B*). Therefore, we conclude that OBP1 and OBP4 do not interact in the presence of 6-MH.

Next we asked whether 6-MH is able to disrupt the interaction between OBP1 and OBP4 that occurs in the presence of indole. For this we prepared the OBP1-indole-OBP4 complex

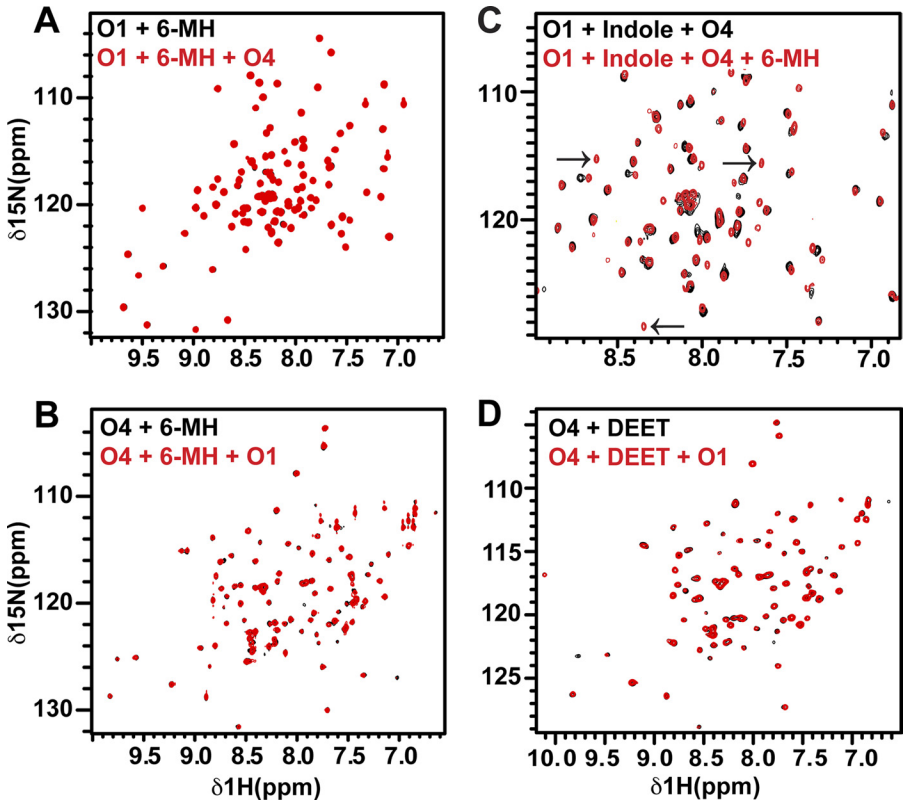

FIGURE 2. **There is no interaction between OBP1 and 4 in the presence of 6-MH.** *A*, ^{1}H-^{15}N HSQC spectrum of ^{15}N-OBP1 (O1) in the presence of 3 mM 6-MH (*black*) overlaid with the spectrum recorded in the presence of OBP4 (O4) (*red*). The spectra are essentially identical, consistent with a lack of interaction between OBP1 and OBP4. *B*, ^{1}H-^{15}N HSQC spectrum of ^{15}N-OBP4 with 3 mM 6-MH (*black*). Addition of OBP1 (*red*) does not result in any chemical shift changes confirming the lack of interaction between the two proteins in the presence of 6-MH. *C*, 6-MH competing with indole for binding to OBP1 in the presence of OBP4. Spectrum of ^{15}N-OBP1 plus indole plus OBP4 (*black*) overlaid with the spectrum of ^{15}N-OBP1 plus indole plus OBP4 plus 6-MH (*red*) is shown. The *black arrows* indicate peaks only observed when OBP1 is bound to 6-MH. *D*, DEET inducing conformational ordering of OBP4 but not allowing interaction between OBP1 and 4. ^{1}H-^{15}N HSQC spectrum of OBP4 in the presence of DEET (*black*) overlaid with the spectrum of OBP4 plus DEET plus OBP1 (*red*) is shown. The lack of shifts indicates no interactions between the two proteins. All spectra were recorded in 20 mM sodium phosphate, pH 7.4, at 25 °C.

using ^{15}N-OBP1 and unlabeled OBP4 and recorded the ^{1}H-^{15}N HSQC spectrum of the complex before and after the addition of 6-MH (Fig. 2*C*). Addition of 6-MH to this sample leads to chemical shift changes and generates a spectrum that is very similar to the spectrum observed for ^{15}N-OBP1–6-MH recorded in the presence of OBP4, where OBP1 and OBP4 do not interact. From this we conclude that 6-MH can compete for binding of indole and disrupt the interaction between OBP1 and 4.

We then asked what effect DEET has on the interactions between OBP1 and OBP4. Using NMR spectroscopy we found that DEET also leads to conformational ordering of OBP4 as seen by the improvement of the OBP4 ^{1}H-^{15}N HSQC spectrum (Fig. 2*D*), and the addition of OBP1 to this complex results in no significant changes, indicating that there is no significant interaction between OBP1 and OBP4 in the presence of DEET (Fig. 2*D*). Therefore, we conclude that DEET and 6-MH can both function to inhibit heterodimerization between OBP1 and OBP4.

NMR Relaxation Studies Show That the OBP1–6MH and OBP1-DEET Complexes Are Monomers in Solution—Previous studies have suggested that because DEET binds at the interface of the OBP1 dimer in the crystal it may act to stabilize formation of the dimeric state of the protein (28). Our previous studies also suggested that OBP1 was predominantly dimeric in the absence of ligand (31). Therefore, we asked whether 6-MH could function to stabilize OBP1-homodimerization. For this, we determined the overall rotational correlation time of the protein from measurements of the ^{15}N NMR relaxation time constants of OBP1 in the presence of 6-MH. The correlation time of a globular protein is directly related to its effective hydrodynamic radius according to the Stokes-Einstein relationship (36) and so directly depends on its oligomerization state. The correlation time of a protein can be calculated directly from the ratio of the longitudinal (T_1) and the transverse (T_2) ^{15}N relaxation time constants for ordered regions of the protein because these are directly dependent on the rotational correlation time according to Equation 1 (36). Therefore, we collected ^{15}N relaxation data for OBP1 in the presence of 6-MH (Fig. 3) and calculated the T_1/T_2 ratios for each amino acid. The average ratio for those residues in well ordered regions of secondary structure was 10.3 ± 1.0 compared with an overall ratio of 10.3 ± 0.5. From Equation 1 this represents an overall correlation time of 9.7 ns. This value is in excellent agreement with the expected value for a monomeric globular protein with a molecular mass of ~14 kDa (36). The dimeric isoform would be expected to have a correlation time in excess of 15 ns (36).

Subsequently, to investigate the dimerization state of OBP1 in the presence of DEET, we obtained a measurement of the

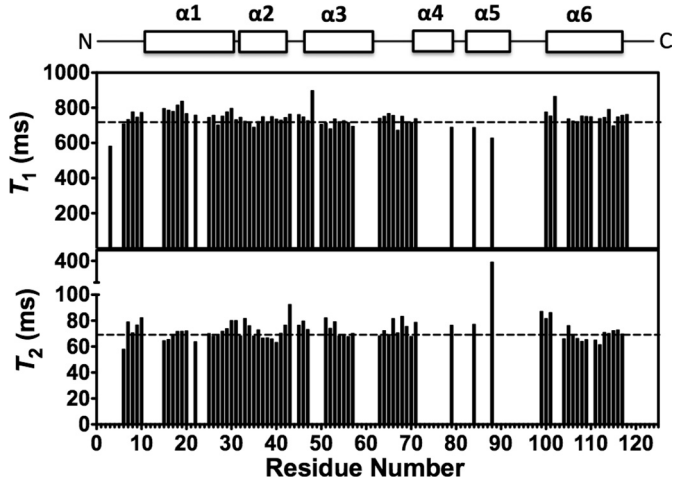

FIGURE 3. **^{15}N NMR relaxation measurements for the OBP1–6MH complex.** ^{15}N T_1 (longitudinal) relaxation times and ^{15}N T_2 (transverse) relaxation times as a function of residue number are shown. The locations of the elements of secondary structure are shown at the *top*. *Dashed lines* represent the mean values of $T_1 = 744.5 \pm 34.7$ ms and $T_2 = 72.6 \pm 6.7$ ms. Values for Thr-3, Asp-48, Lys-50, and Ala-88 were excluded from these calculations because their T_2 values deviated significantly from the mean. Spectra were recorded in 20 mM sodium phosphate, pH 7.4, at 25 °C. Assignments were extrapolated from those made with OBP1-indole; only unambiguous peaks were assigned.

correlation time from an analysis of the global T_1 and T_2 values determined using one-dimensional versions of the ^{15}N relaxation experiments used for OBP1–6MH complexes. Fitting the total integrated signal intensities of the backbone amide ^{1}H region of a one-dimensional spectrum OBP1-DEET as a function of delay times to an exponential decay gave an average T_1/T_2 ratio of 10.9 ± 0.5 s. This equates to an overall correlation time for the OBP-1-DEET complex of 10.0 ns, which is in excellent agreement with the value obtained from the full analysis of the OBP1–6-MH T_1 and T_2 relaxation times. This is consistent with OBP1 existing in the monomeric form in the presence of DEET.

From the NMR relaxation experiments, we conclude that in the presence of either 6-MH or DEET, OBP1 is monomeric in solution and that these repellents do not disrupt the interaction between OBP1 and OBP4 by stabilizing the dimeric state of OBP1. Rather, this suggests that they must either directly disrupt binding of OBP4 by binding at the OBP1-OBP4 interface or alternatively by inducing specific conformational changes that are different from those induced by the binding of indole and that do not allow formation of the OBP1-OBP4 complex.

Binding Affinities of OBP4 and OBP1 for Ligands—Previous work has established the use of fluorescence-based competition binding assays to discover high affinity ligands for OBPs (48). These assays are based on the ability of candidate ligands to displace a fluorescent reporter, typically 1-NPN, from the central binding pocket. 1-NPN is a hydrophobic dye that exhibits a large blue shift and increase in fluorescence intensity when bound to the hydrophobic pocket of OBPs. We used this approach to determine the binding affinities of 6-MH, indole, and DEET to OBP1 and OBP4. Initially, for OBP1 we measured a K_D for 1-NPN of 2.63 ± 0.32 μM, and for OBP4 we measured a K_D of 0.55 ± 0.04 μM. Whereas the value obtained for OBP1 is in close agreement with published values, the value obtained for OBP4 is significantly lower than the previously reported value (30).

It has previously been shown that 6-MH is ineffective at fully displacing 1-NPN from OBP1 (30). We confirmed this result (Fig. 4*A*), which shows that a 200-fold molar excess of either 6-MH, DEET, or indole does not compete for binding of 1-NPN and produces at best a 50% reduction in the fluorescence intensity of 1-NPN. Fitting the curves to a simple single site model of binding gives EC_{50} values for 6-MH, 6.56 ± 1.62 μM; DEET, 41.39 ± 1.83 μM; and indole, 11.19 ± 1.44 μM. However, the shape of these curves, which shows an initial steep decline followed by a long linear tail, suggests that binding of these three ligands is not competitive with 1-NPN binding. To validate this, we used an alternative approach and determined the K_D of 1-NPN for OBP1 in the presence of increasing concentrations of 6-MH (Fig. 4*B*). In these experiments we saw no change in the resulting 1-NPN binding curve with increasing concentrations of 6-MH, indicating that 6-MH does not compete for 1-NPN. Assays performed with indole (Fig. 4*D*) and DEET (Fig. 4*E*) show similar results. Therefore, we conclude that 6-MH and DEET must bind simultaneously with 1-NPN to OBP1 and that the observed change in 1-NPN fluorescence is a result of fluorescence quenching rather than as a result of the displacement of 1-NPN. In support of this, the crystal structures of both the OBP1–6-MH and OBP1-DEET complexes (Fig. 1, *B* and *C*) show that these ligands bind at the periphery of the central binding pocket, and in both cases a PEG molecule occupies the central cavity. Our fluorescence data strongly suggest that 1-NPN must also be able to bind in this cavity at the same time that 6-MH or DEET binds to the periphery.

In contrast to 6-MH and DEET, experiments performed with citronellal are fundamentally different. In competition binding experiments citronellal almost completely abolishes 1-NPN fluorescence with an $EC_{50} = 1.89 \pm 0.43$ μM (Fig. 4*A*), whereas in heterologous binding assays, there is a rightward shift in the binding curve with increasing concentrations of citronellal (Fig. 4*C*), indicative of competitive binding. Simultaneously fitting these curves to Equation 2 yields a K_i of 1.40 ± 0.12 μM. Using the Cheng-Prusoff relationship (Equation 5) to convert the measured EC_{50} values determined from data shown in Fig. 4*A* yields a similar value of $K_i = 2.44 \pm 0.22$ μM.

Similar results were obtained for 1-NPN displacement binding assays performed with OBP4 giving EC_{50} values of 6-MH = 3.5 ± 0.8 μM; DEET, 103.8 ± 2.7 μM; and indole, 36.4 ± 2.5 μM (Fig. 5*A*). Analogous to OBP1, heterologous binding assays show that indole DEET and 6-MH have little or no effect on the K_D for 1-NPN (Fig. 5*B*); so we conclude that binding of these ligands to OBP4 is again not competitive with 1-NPN and thus K_i values cannot be calculated using the Cheng-Prusoff relationship.

ANS Ligand Displacement Assays—As the results from the 1-NPN displacement assays, with the exception of citronellal, could not be used to measure binding affinities because of the noncompetitive nature of the interactions, we investigated the use of ANS to obtain K_i values. In these experiments the binding of ANS to OBP1 was too weak and the distortions from the inner filter effect at the high concentrations of ANS required (>200 μM), precluded further analysis. In contrast, the binding

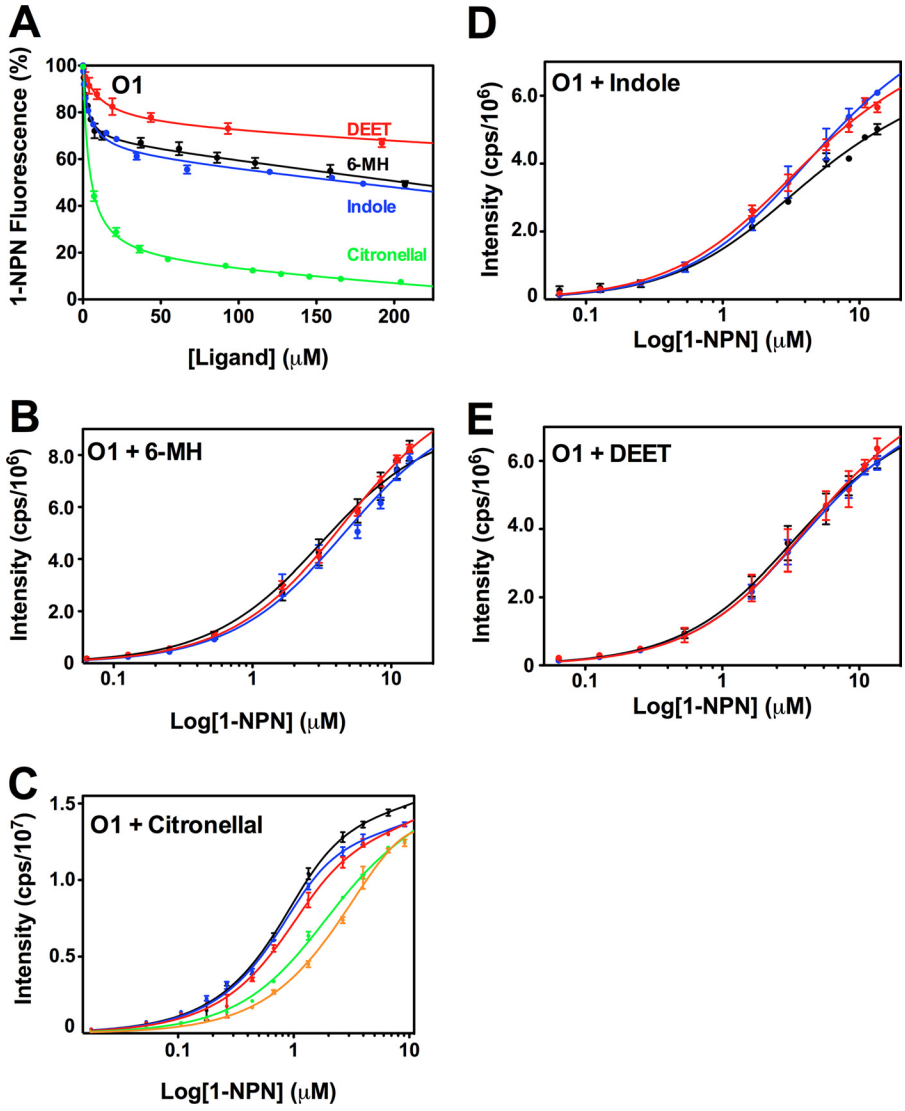

FIGURE 4. **Assay of OBP1 binding to 1-NPN in the presence of 6-MH, DEET, indole, and citronellal.** *A*, competition binding assay. OBP1 (O1) in the presence of 1-NPN (both 1 μM in 50 mM Tris-HCl, pH 7.4) was titrated with 6-MH (*black*), DEET (*red*), indole (*blue*), or citronellal (*green*) to final concentrations of ~200 μM. Fluorescence intensity is normalized to the value in the absence of ligand. *B*, heterologous binding assay revealing that 6-MH does not compete with 1-NPN binding. OBP1 (1 μM) in the absence (*black*) or presence of 6-MH (50 μM, *blue*; 200 μM, *red*) was titrated with 1-NPN to a final concentration of 13 μM. *C*, citronellal competing for binding of 1-NPN. OBP1 in the absence (*black*) or presence of citronellal (5 μM, *red*; 10 μM, *blue*; 50 μM, *green*; or 100 μM, *orange*) was titrated with 1-NPN to a final concentration of 11 μM. *D*, DEET and indole not competing with 1-NPN for OBP1 binding. Log plots of OBP1 titrated with 1-NPN to a final concentration of 13.5 μM, in the absence (*black*) or presence of DEET (20 μM, *red*; 100 μM, *blue*) are shown. *E*, as in *D* with indole as opposed to DEET. 1-NPN and ligand solutions were in methanol, and all curves are an average of three replicates, and *error bars* are shown. In *B*--*E*, OBP1 was 1 μM in 50 mM Tris-HCl, pH 7.4, and the concentration of 1-NPN was 1 mM in methanol.

affinity of ANS for OBP4 was significantly higher (K_D = 8.2 ± 1.5 μM). To verify that binding of ligands to OBP4 directly competes for binding of 1,8-ANS we again performed heterologous binding assays of 1,8-ANS in the presence of increasing concentrations of the respective ligand. These experiments confirmed that binding was directly competitive, as exemplified by the rightward shift of the binding curves (Fig. 5*D*) and from double reciprocal Lineweaver-Burk plots which intercept the *y* axis at the same value (Fig. 5*D*, *inset*). Similar results are obtained with DEET and indole (Fig. 5, *E* and *F*). Therefore, from 1,8-ANS displacement assays with OBP4 we obtained K_i values for 6-MH of 326 ± 7 μM, DEET 53.1 ± 2.4 μM, and indole 137.1 ± 2.2 μM (Fig. 5*C*), and these are in agreement with the values obtained the heterologous binding assays that gave values for 6-MH of 272 ± 5 μM, DEET 64.5 ± 6.4 μM, and indole 148.1 ± 2.2 μM.

DISCUSSION

A. gambiae OBP1 binds the human sweat component 6-MH at the same site as the synthetic repellent DEET. The fact that two compounds with repellent properties but different chemical composition bind to the same site, and both components disrupt heterodimeric interactions formed in the presence of known biologically relevant odorants suggests that this binding site may be an important site for the action of multiple repellent compounds.

OBP1 and 4 require indole for heterodimerization, but 6-MH, despite being able to induce conformational ordering of OBP4 and bind to both OBP1 and OBP4, does not induce heterodimerization. DEET has been proposed to stabilize the OBP1 homodimer (28), which may prevent heterodimerization

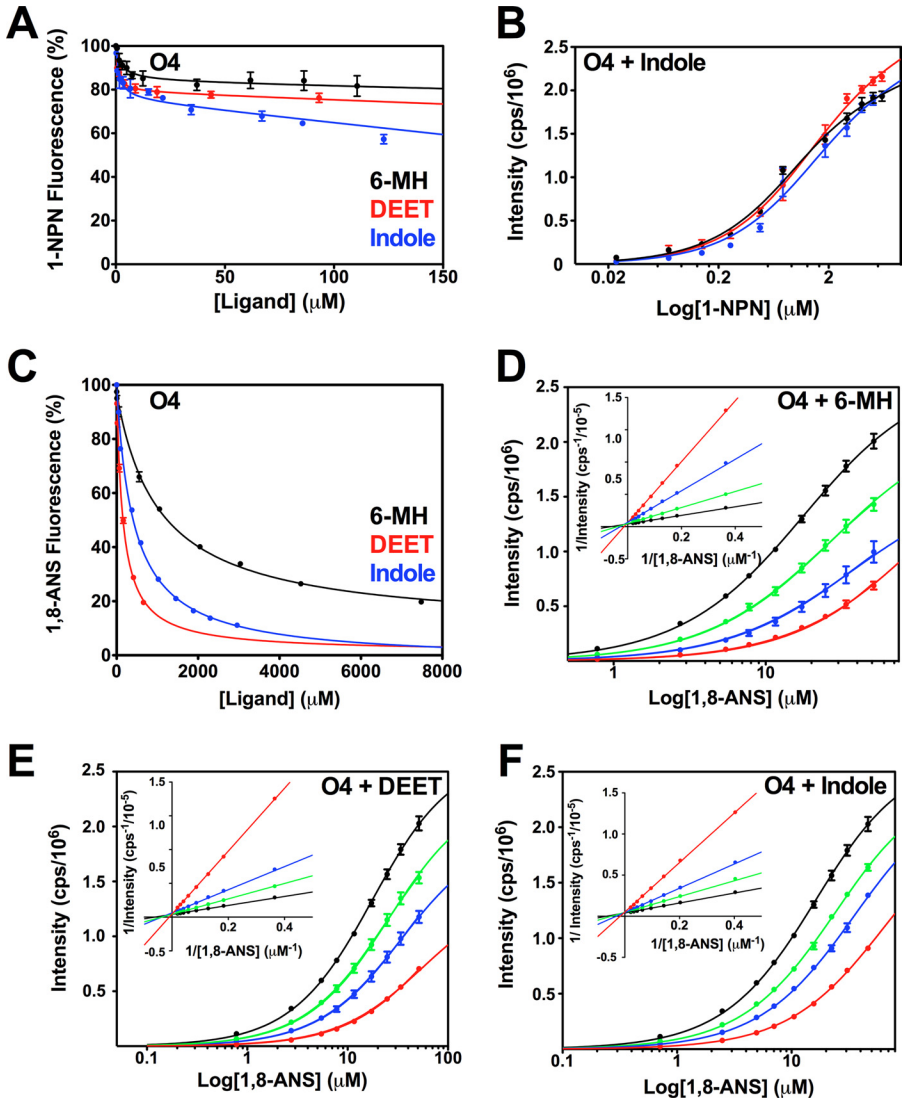

FIGURE 5. **Assay of 6-MH, DEET, and indole binding to OBP4.** *A*, 6-MH, DEET, and indole do not displace 1-NPN from OBP4 (O4). OBP4 in the presence of 1-NPN (both 0. 5 μM in 50 mM Tris-HCl, pH 7.4) was titrated with a 10 mM 6-MH (*black*), 10 mM DEET (*red*), or 10 mM indole (*blue*) to final concentrations of ≈200 μM. Fluorescence intensity is normalized to the value in the absence of ligand. *B*, indole does not compete for 1-NPN binding: OBP4 (0.5 μM) in the absence (*black*) or presence of indole (5 μM, *blue*; 50 μM, *red*) was titrated with 1-NPN (1 mM) to a final concentration of 6 μM. *C*, increasing concentrations of 6-MH (*black*), DEET (*red*), and indole (*blue*) can displace 1,8-ANS (20 μM) from OBP4 (5 μM). Fluorescence intensity is displayed as percentage of the value in the absence of ligand. *D–F*, log plots of 1,8-ANS titrations into OBP4 (5 μM in 50 mM Tris-HCl, pH 7.4) is shown in the absence (*black*) or presence of (*D*) 6-MH, 500 μM (*green*), 1000 μM (*blue*), or 5000 μM (*red*); (*E*) DEET, 100 μM (*green*), 200 μM (*blue*), or 500 μM (*red*); (*F*) indole, 235 μM (*green*), 470 μM (*blue*), or 1088 μM (*red*). The Lineweaver-Burk plots (*insets* in *D–F*) are linear and intercept the *y* axis at the same point showing competitive binding in each case. All ligands were added as solutions in methanol to a maximum methanol concentration of 1%. Each curve is the average of three replicates and *error bars* are shown; these are within the limits of the symbol for the Lineweaver-Burk plots.

between OBP1 and 4. However, the NMR relaxation studies presented here clearly establish that OBP1 is monomeric in the presence of 6-MH and DEET, indicating that these repellents must block the interaction with OBP4 through some other mechanism (Fig. 6). 6-MH and DEET bind in an opening between helices 4 and 5 of OBP1, with one end of the molecule projecting into solution at the interface of the OBP1 crystal dimer. Our previous studies of the OBP1-OBP4 interactions identified a distinct conformational change in OBP4 induced by binding of indole that was required to stabilize a binding site for OBP1 (31). However, our findings with OBP1 were less clear. NMR provided evidence of a site of interaction for OBP4 involving helices 1, 3, and 4 of OBP1. Unfortunately, a number of residues in helices 4 and 5 of OBP1 could not be observed in the NMR spectrum of the OBP1-indole complex, and because of this we could not directly determine whether an interaction occurred with OBP4 in this region (31). Therefore, we cannot rule out that 6-MH and DEET binding disrupts the interaction with OBP4 by preventing an interaction at an interface that involves helices 4 and 5. Alternatively, because conformational changes induced by ligand binding are required for the interaction of OBP4 with OBP1, an alternative explanation is that 6-MH (and DEET) binding results in conformational changes significantly different from those induced by indole, perhaps in OBP4, which prevent heterodimerization. Efforts to determine the crystal structure of OBP4 with 6-MH have so far proved unsuccessful.

6-MH and DEET both inhibit OBP1-OBP4 heterodimerization, and 6-MH competes for binding of indole (Fig. 6). It has

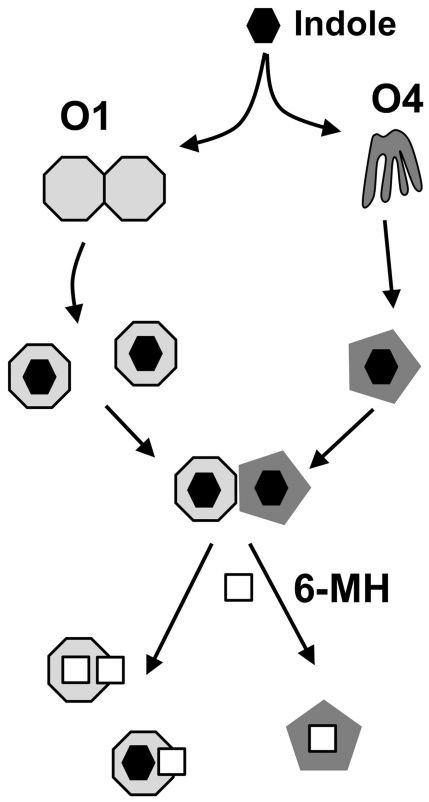

FIGURE 6. **Scheme of ligand and repellent binding to OBP1 and 4.** In the absence of ligands OBP1 (*light gray octagon*) appears to exist predominantly as dimers, whereas OBP4 (*dark gray*) is a highly dynamic structure. Binding of odorants, including indole (*black*), leads to dissociation of OBP1 into monomers and a stabilization of the OBP4 structure that allows the two proteins to form heterodimers. Repellent molecules, like 6-MH (*white square*) can function either to compete for and displace the normal ligand or can bind at the same time as the native ligand and disrupt the formation of the OBP1-OBP4 complex.

been shown that DEET blocks electrophysiological responses of olfactory sensory neurons to attractive odors (25), and this could be due to competitive interactions by repellents (25, 49). Whereas other studies provide evidence that insects actively sense and respond to DEET (27), the present and previous studies also suggest that DEET and other repellents may target OBP function by either disrupting interactions with natural ligands or preventing interactions with other components of the olfactory signaling pathway.

Our reanalysis of 6-MH and DEET binding using 1-NPN displacement assays shows that these ligands do not compete for 1-NPN binding to OBP1; rather, they bind to OBP1 at the same time as 1-NPN and quench its fluorescence. It has previously been reported that K_i values obtained from such assays do not correlate well with affinity values determined by other methods (50) or with behavioral or electrophysiological responses (20, 51) and that behavioral responses to mixtures of compounds are known to be different from the response to their components alone (52). From the structure presented here and previously published structures (53), it is apparent that multiple ligands can bind to some OBPs at the same time. This presents the possibility that it may be the combination of different ligands bound to a single OBP that is necessary to form the correct conformation or that certain OBP-ligand complexes are required to form heterodimers to elicit a response.

The present data add support for the hypothesis (20, 29, 54) that it is the specific conformation induced by binding of ligand and the effect that this has on the interactions of the OBP-ligand complex with other components of the olfactory system that may be important for activity, rather than the binding affinity for a specific ligand. In particular, a number of efforts are underway to discover novel modulators of OBP function to disrupt normal insect behavior. Our findings with 6-MH and DEET have significant implications for discovery efforts based on competition binding assays. Whereas such efforts may be extremely powerful in defining ligands that bind with high affinity to a specific OBP, the present result, which reveals that 6-MH and DEET bind to the same site in OBP1 but fail to compete for a reporter, suggests that using binding affinity alone as a marker of activity can overlook highly effective repellents. This suggests that an approach that seeks to identify the odorant response profile for a particular OBP, as has been done for OBP1, and understanding the specific conformational changes induced by ligands and how this affects interactions with other components of the olfactory system may provide a more fruitful approach to rationally discover novel modulators of OBP functions and ultimately mosquito behavior.

Acknowledgments—We thank Dr. Jay Nix for assistance in x-ray data collection; and Patrick Jones, Jason Pitts, and Dr. Larry Zwiebel for A. gambiae cDNA libraries. Operation of the x-ray crystallography and NMR spectroscopy facilities at University of Colorado School of Medicine is supported by the Program in Structural Biology and Biophysics, and the University of Colorado Cancer Center (National Institutes of Health Grant P30-CA046934).

REFERENCES

1. Crawford, J. E., and Lazzaro, B. P. (2010) The demographic histories of the M and S molecular forms of *Anopheles gambiae* s.s. *Mol. Biol. Evol.* **27,** 1739–1744
2. Dondorp, A. M., Nosten, F., Yi, P., Das, D., Phyo, A. P., Tarning, J., Lwin, K. M., Ariey, F., Hanpithakpong, W., Lee, S. J., Ringwald, P., Silamut, K., Imwong, M., Chotivanich, K., Lim, P., Herdman, T., An, S. S., Yeung, S., Singhasivanon, P., Day, N. P., Lindegardh, N., Socheat, D., and White, N. J. (2009) Artemisinin resistance in *Plasmodium falciparum* malaria. *New Engl. J. Med.* **361,** 455–467
3. RTSS Clinical Trials Partnership (2012) A phase 3 trial of RTS,S/AS01 malaria vaccine in African infants. *New Engl. J. Med.* **367,** 2284–2295
4. Trape, J. F., and Rogier, C. (1996) Combating malaria morbidity and mortality by reducing transmission. *Parasitol. Today* **12,** 236–240
5. Hallem, E. A., Nicole Fox, A., Zwiebel, L. J., and Carlson, J. R. (2004) Olfaction: mosquito receptor for human-sweat odorant. *Nature* **427,** 212–213
6. Mukabana, W. R., Takken, W., Coe, R., and Knols, B. G. (2002) Host-specific cues cause differential attractiveness of Kenyan men to the African malaria vector *Anopheles gambiae*. *Malaria J.* **1,** 17
7. Knols, B. G., de Jong, R., and Takken, W. (1995) Differential attractiveness of isolated humans to mosquitoes in Tanzania. *Trans. R. Soc. Trop. Med. Hyg.* **89,** 604–606
8. Skinner, W. A., Tong, H., Pearson, T., Strauss, W., and Maibach, H. (1965) Human sweat components attractive to mosquitoes. *Nature* **207,** 661–662
9. Logan, J. G., Birkett, M. A., Clark, S. J., Powers, S., Seal, N. J., Wadhams, L. J., Mordue Luntz, A. J., and Pickett, J. A. (2008) Identification of human-derived volatile chemicals that interfere with attraction of *Aedes aegypti* mosquitoes. *J. Chem. Ecol.* **34,** 308–322
10. Logan, J. G., Stanczyk, N. M., Hassanali, A., Kemei, J., Santana, A. E.,

Ribeiro, K. A., Pickett, J. A., and Mordue Luntz, A. J. (2010) Arm-in-cage testing of natural human-derived mosquito repellents. *Malaria J.* **9,** 239
11. Maia, M. F., and Moore, S. J. (2011) Plant-based insect repellents: a review of their efficacy, development and testing. *Malaria J.* **10,** S11
12. Vogt, R. G. (2003) Biochemical diversity of odor detection: OBPs, ODEs and SNMPs. in *Insect Pheromone Biochemistry and Molecular Biology* (Blomquist, G. J., and Vogt, R. G., eds) pp. 391–446, Elsevier, London
13. Vogt, R. G., Köhne, A. C., Dubnau, J. T., and Prestwich, G. D. (1989) Expression of pheromone binding proteins during antennal development in the gypsy moth *Lymantria dispar*. *J. Neurosci.* **9,** 3332–3346
14. Sandler, B. H., Nikonova, L., Leal, W. S., and Clardy, J. (2000) Sexual attraction in the silkworm moth: structure of the pheromone-binding-protein-bombykol complex. *Chem. Biol.* **7,** 143–151
15. Horst, R., Damberger, F., Luginbühl, P., Güntert, P., Peng, G., Nikonova, L., Leal, W. S., and Wüthrich, K. (2001) NMR structure reveals intramolecular regulation mechanism for pheromone binding and release. *Proc. Natl. Acad. Sci. U.S.A.* **98,** 14374–14379
16. Wojtasek, H., and Leal, W. (1999) Conformational change in the pheromone-binding protein from *Bombyx mori* induced by pH and by interaction with membranes. *J. Biol. Chem.* **274,** 30950–30956
17. Damberger, F. F., Ishida, Y., Leal, W. S., and Wüthrich, K. (2007) Structural basis of ligand binding and release in insect pheromone-binding proteins: NMR structure of *Antheraea polyphemus* PBP1 at pH 4.5. *J. Mol. Biol.* **373,** 811–819
18. Zubkov, S., Gronenborn, A. M., Byeon, I. J., and Mohanty, S. (2005) Structural consequences of the pH-induced conformational switch in *A. polyphemus* pheromone-binding protein: mechanisms of ligand release. *J. Mol. Biol.* **354,** 1081–1090
19. Xu, P., Atkinson, R., Jones, D. N., and Smith, D. P. (2005) *Drosophila* OBP LUSH is required for activity of pheromone-sensitive neurons. *Neuron* **45,** 193–200
20. Laughlin, J. D., Ha, T. S., Jones, D. N., and Smith, D. P. (2008) Activation of pheromone-sensitive neurons is mediated by conformational activation of pheromone-binding protein. *Cell* **133,** 1255–1265
21. Ronderos, D. S., and Smith, D. P. (2010) Activation of the T1 neuronal circuit is necessary and sufficient to induce sexually dimorphic mating behavior in *Drosophila melanogaster*. *J. Neurosci.* **30,** 2595–2599
22. Katz, T. M., Miller, J. H., and Hebert, A. A. (2008) Insect repellents: historical perspectives and new developments. *J. Am. Acad. Dermatol.* **58,** 865–871
23. Briassoulis, G., Narlioglou, M., and Hatzis, T. (2001) Toxic encephalopathy associated with use of DEET insect repellents: a case analysis of its toxicity in children. *Hum. Exp. Toxicol.* **20,** 8–14
24. Rutledge, L. C., Moussa, M. A., Lowe, C. A., and Sofield, R. K. (1978) Comparative sensitivity of mosquito species and strains to the repellent diethyl toluamide. *J. Med. Entomol.* **14,** 536–541
25. Ditzen, M., Pellegrino, M., and Vosshall, L. B. (2008) Insect odorant receptors are molecular targets of the insect repellent DEET. *Science* **319,** 1838–1842
26. Pellegrino, M., Steinbach, N., Stensmyr, M. C., Hansson, B. S., and Vosshall, L. B. (2011) A natural polymorphism alters odour and DEET sensitivity in an insect odorant receptor. *Nature* **478,** 511–514
27. Syed, Z., and Leal, W. S. (2008) Mosquitoes smell and avoid the insect repellent DEET. *Proc. Natl. Acad. Sci. U.S.A.* **105,** 13598–13603
28. Tsitsanou, K. E., Thireou, T., Drakou, C. E., Koussis, K., Keramioti, M. V., Leonidas, D. D., Eliopoulos, E., Iatrou, K., and Zographos, S. E. (2012) *Anopheles gambiae* odorant-binding protein crystal complex with the synthetic repellent DEET: implications for structure-based design of novel mosquito repellents. *Cell. Mol. Life Sci.* **69,** 283–297
29. Biessmann, H., Andronopoulou, E., Biessmann, M. R., Douris, V., Dimitratos, S. D., Eliopoulos, E., Guerin, P. M., Iatrou, K., Justice, R. W., Kröber, T., Marinotti, O., Tsitoura, P., Woods, D. F., and Walter, M. F. (2010) The *Anopheles gambiae* odorant-binding protein 1 (AgamOBP1) mediates indole recognition in the antennae of female mosquitoes. *PLoS ONE* **5,** e9471
30. Qiao, H., He, X., Schymura, D., Ban, L., Field, L., Dani, F. R., Michelucci, E., Caputo, B., della Torre, A., Iatrou, K., Zhou, J. J., Krieger, J., and Pelosi, P. (2011) Cooperative interactions between odorant-binding proteins of *Anopheles gambiae*. *Cell. Mol. Life Sci.* **68,** 1799–1813
31. Davrazou, F., Dong, E., Murphy, E. J., Johnson, H. T., and Jones, D. N. (2011) New insights into the mechanism of odorant detection by the malaria-transmitting mosquito *Anopheles gambiae*. *J. Biol. Chem.* **286,** 34175–34183
32. Kruse, S. W., Zhao, R., Smith, D. P., and Jones, D. N. (2003) Structure of a specific alcohol-binding site defined by the odorant-binding protein LUSH from *Drosophila melanogaster*. *Nat. Struct. Biol.* **10,** 694–700
33. Thode, A. B., Kruse, S. W., Nix, J. C., and Jones, D. N. (2008) The role of multiple hydrogen-bonding groups in specific alcohol binding sites in proteins: insights from structural studies of LUSH. *J. Mol. Biol.* **376,** 1360–1376
34. Fogh, R., Ionides, J., Ulrich, E., Boucher, W., Vranken, W., Linge, J. P., Habeck, M., Rieping, W., Bhat, T. N., Westbrook, J., Henrick, K., Gilliland, G., Berman, H., Thornton, J., Nilges, M., Markley, J., and Laue, E. (2002) The CCPN project: an interim report on a data model for the NMR community. *Nat. Struct. Biol.* **9,** 416–418
35. Vranken, W. F., Boucher, W., Stevens, T. J., Fogh, R. H., Pajon, A., Llinas, M., Ulrich, E. L., Markley, J. L., Ionides, J., and Laue, E. D. (2005) The CCPN data model for NMR spectroscopy: development of a software pipeline. *Proteins* **59,** 687–696
36. Rossi, P., Swapna, G. V., Huang, Y. J., Aramini, J. M., Anklin, C., Conover, K., Hamilton, K., Xiao, R., Acton, T. B., Ertekin, A., Everett, J. K., and Montelione, G. T. (2010) A microscale protein NMR sample screening pipeline. *J. Biomol. NMR* **46,** 11–22
37. Farrow, N. A., Muhandiram, R., Singer, A. U., Pascal, S. M., Kay, C. M., Gish, G., Shoelson, S. E., Pawson, T., Forman-Kay, J. D., and Kay, L. E. (1994) Backbone dynamics of a free and phosphopeptide-complexed Src homology 2 domain studied by ^{15}N NMR relaxation. *Biochemistry* **33,** 5984–6003
38. Pflugrath, J. W. (1999) The finer things in x-ray diffraction data collection. *Acta Crystallogr. D Biol. Crystallogr.* **55,** 1718–1725
39. McCoy, A. J., Grosse-Kunstleve, R. W., Storoni, L. C., and Read, R. J. (2005) Likelihood-enhanced fast translation functions. *Acta Crystallogr. D Biol. Crystallogr.* **61,** 458–464
40. Collaborative Computational Project, Number 4 (1994) Programs for protein crystallography. *Acta Crystallogr. D Biol. Crystallogr.* **50,** 760–763
41. Murshudov, G. N., Vagin, A. A., and Dodson, E. J. (1997) Refinement of macromolecular structures by the maximum-likelihood method. *Acta Crystallogr. D Biol. Crystallogr.* **53,** 240–255
42. Emsley, P., and Cowtan, K. (2004) COOT: model-building tools for molecular graphics. *Acta Crystallogr. D Biol. Crystallogr.* **60,** 2126–2132
43. Swillens, S. (1995) Interpretation of binding curves obtained with high receptor concentrations: practical aid for computer analysis. *Mol. Pharmacol.* **47,** 1197–1203
44. Spinelli, S., Lagarde, A., Iovinella, I., Legrand, P., Tegoni, M., Pelosi, P., and Cambillau, C. (2012) Crystal structure of *Apis mellifera* OBP14, a C-minus odorant-binding protein, and its complexes with odorant molecules. *Insect Biochem. Mol. Biol.* **42,** 41–50
45. Lartigue, A., Gruez, A., Spinelli, S., Rivière, S., Brossut, R., Tegoni, M., and Cambillau, C. (2003) The crystal structure of a cockroach pheromone-binding protein suggests a new ligand binding and release mechanism. *J. Biol. Chem.* **278,** 30213–30218
46. Wogulis, M., Morgan, T., Ishida, Y., Leal, W. S., and Wilson, D. K. (2006) The crystal structure of an odorant-binding protein from *Anopheles gambiae*: evidence for a common ligand release mechanism. *Biochem. Biophys. Res. Commun.* **339,** 157–164
47. Bucci, B. K., Kruse, S. W., Thode, A. B., Alvarado, S. M., and Jones, D. N. (2006) Effect of *n*-alcohols on the structure and stability of the *Drosophila* odorant-binding protein LUSH. *Biochemistry* **45,** 1693–1701
48. Ban, L., Zhang, L., Yan, Y., and Pelosi, P. (2002) Binding properties of a locust's chemosensory protein. *Biochem. Biophys. Res. Commun.* **293,** 50–54
49. Davis, E. E. (1985) Insect repellents: concepts of their mode of action relative to potential sensory mechanisms in mosquitoes (Diptera: Culicidae). *J. Med. Entomol.* **22,** 237–243
50. Gong, Y., and Plettner, E. (2011) Effects of aromatic compounds on antennal responses and on the pheromone-binding proteins of the gypsy

moth (*Lymantria dispar*). *Chem. Senses* **36,** 291–300
51. Honson, N., Johnson, M. A., Oliver, J. E., Prestwich, G. D., and Plettner, E. (2003) Structure-activity studies with pheromone-binding proteins of the gypsy moth, *Lymantria dispar*. *Chem. Senses* **28,** 479–489
52. Qiu, Y. T., Smallegange, R. C., Hoppe, S., van Loon, J. J., Bakker, E. J., and Takken, W. (2004) Behavioural and electrophysiological responses of the malaria mosquito *Anopheles gambiae* Giles sensu stricto (Diptera: Culicidae) to human skin emanations. *Med. Vet. Entomol.* **18,** 429–438
53. Lautenschlager, C., Leal, W. S., and Clardy, J. (2007) *Bombyx mori* pheromone-binding protein binding nonpheromone ligands: implications for pheromone recognition. *Structure* **15,** 1148–1154
54. Ziemba, B. P., Murphy, E. J., Edlin, H. T., and Jones, D. N. (2013) A novel mechanism of ligand binding and release in the odorant-binding protein 20 from the malaria mosquito Anopheles gambiae. *Protein Sci.* **22,** 11–21